

Sometimes Painful but Certainly Promising: Feasibility and Trade-offs of Language Model Inference at the Edge

MAXIMILIAN ABSTREITER, University of Helsinki, Finland

SASU TARKOMA, University of Helsinki, Finland

ROBERTO MORABITO, EURECOM, France and University of Helsinki, Finland

The rapid rise of Language Models (LMs) has expanded the capabilities of natural language processing, powering applications from text generation to complex decision-making. While state-of-the-art LMs often boast hundreds of billions of parameters and are primarily deployed in data centers, recent trends show a growing focus on compact models—typically under 10 billion parameters—enabled by techniques such as quantization and other model compression techniques. This shift paves the way for LMs on edge devices, offering potential benefits such as enhanced privacy, reduced latency, and improved data sovereignty. However, the inherent complexity of even these smaller models, combined with the limited computing resources of edge hardware, raises critical questions about the practical trade-offs in executing LM inference outside the cloud. To address these challenges, we present a comprehensive evaluation of generative LM inference on representative CPU-based and GPU-accelerated edge devices. Our study measures key performance indicators—including memory usage, inference speed, and energy consumption—across various device configurations. Additionally, we examine throughput-energy trade-offs, cost considerations, and usability, alongside an assessment of qualitative model performance. While quantization helps mitigate memory overhead, it does not fully eliminate resource bottlenecks, especially for larger models. Our findings quantify the memory and energy constraints that must be considered for practical real-world deployments, offering concrete insights into the trade-offs between model size, inference performance, and efficiency. The exploration of LMs at the edge is still in its early stages. We hope this study provides a foundation for future research, guiding the refinement of models, the enhancement of inference efficiency, and the advancement of edge-centric AI systems.

CCS Concepts: • **Computing methodologies** → **Natural language generation**; • **General and reference** → **Performance; Evaluation**; • **Hardware** → **Power and energy**; • **Computer systems organization** → *Distributed architectures*.

Key words and phrases: Edge AI, Small Language Models (SLMs), Large Language Models (LLMs), On-Device AI, Generative AI, Benchmarking

1 Introduction

Language models (LMs) have gained significant attention in recent years, particularly following the launch of the ChatGPT service in autumn 2022 [47].

Beyond their role in conversational AI and virtual assistants, these models are driving substantial transformations across multiple industries, including healthcare, education, entertainment, and software development [6, 37, 43, 54]. Leading-edge models like GPT-4o have established new benchmarks for AI performance, excelling in general knowledge evaluation (MMLU), mathematical reasoning (GSM8K), and code

Authors' Contact Information: [Maximilian Abstreiter](mailto:maximilian.abstreiter@helsinki.fi), maximilian.abstreiter@helsinki.fi, University of Helsinki, Department of Computer Science, Helsinki, Finland; [Sasu Tarkoma](mailto:sasu.tarkoma@helsinki.fi), sasutarkoma@helsinki.fi, University of Helsinki, Department of Computer Science, Helsinki, Finland; [Roberto Morabito](mailto:roberto.morabito@eurecom.fr), roberto.morabito@eurecom.fr, EURECOM, Communication Systems Department, Sophia Antipolis, France and University of Helsinki, Department of Computer Science, Helsinki, Finland.

2025. This paper is currently under review for publication in an ACM journal. If accepted, the copyright will be transferred to ACM.

generation (HumanEval), while also supporting multimodal interactions [34]. Even fields such as IoT and edge computing are already integrating or preparing to adopt these advanced technologies. These advancements come, however, with significant computational and storage demands, which are primarily managed through cloud-based infrastructures. While cloud-hosted inference provides scalability and centralized optimization, it also introduces challenges such as increased network latency, data privacy concerns, and high operational costs.

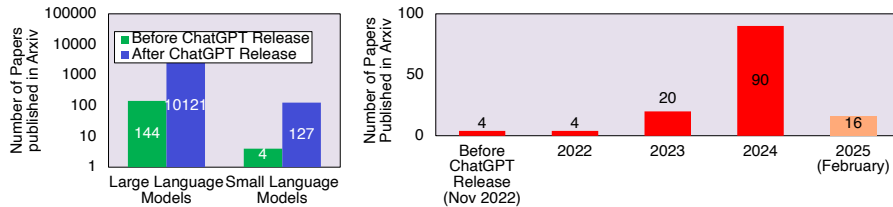


Fig. 1. Comparison of the number of research papers published on arXiv mentioning 'Large Language Models' (LLMs) and 'Small Language Models' (SLMs) in their title before and after the release of ChatGPT, illustrating the rising research interest in edge-optimized AI models.

To address these issues, there is a growing trend toward deploying LMs at the edge, paralleling earlier shifts in AI inference from centralized data centers to resource-constrained, decentralized environments. Similar to pre-LM AI workloads, efforts to enable LM execution closer to the edge are driven by the need to reduce latency, enhance reliability, and improve user experiences. This growing interest in smaller-scale models is also reflected in the research community. As shown in Figure 1, the number of papers published on arXiv mentioning "Large Language Model" in their titles skyrocketed from 184 (over a decade) to 8,480 in just a few years after ChatGPT's release. While work on Small Language Models (SLMs) remains a more niche area, its trajectory follows a similar trend, with research output rising from just 4 papers before ChatGPT's release to over 126 in early 2025. This indicates that SLMs are becoming a significant research focus, aligning with the broader push toward efficient, resource-constrained AI models. It is important to note that there is no strict definition of what differentiates an LLM from an SLM in terms of parameter count. While LLMs often exceed tens or even hundreds of billions of parameters, SLMs typically remain under 10 billion, though this boundary is not universally defined. Nevertheless, the trend toward optimizing models for edge and mobile deployment is clear, reinforcing the need to investigate the feasibility of running LMs on resource-constrained devices.

Despite this increasing interest in edge-centric LMs, however, the question remains: *to what extent can resource-constrained devices efficiently execute LM inference?*

Recent advances in model compression [55], such as quantization and knowledge distillation, have enabled the development of more efficient LMs for edge and mobile environments. While quantization reduces memory and computational requirements by lowering parameter precision, distillation transfers knowledge to smaller models with fewer parameters, making them more suitable for resource-constrained settings. Examples include Phi-3.5 [1], Llama 3.2 [4], and a variety of emerging mobile-optimized LMs. In this respect, the rapid rise of these compact models reflects a broader shift toward efficient, resource-aware AI, as shown

in Figure 2, which illustrates the increasing number of sub-4B models releases over recent years—we focus on sub-4B models to maintain clarity, as including larger models would make the visualization overly crowded.

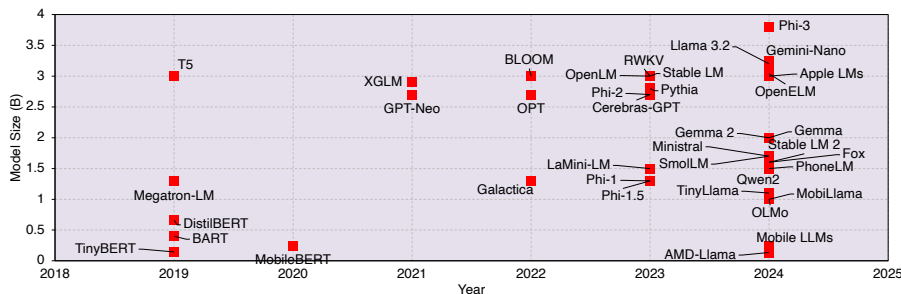


Fig. 2. Growth of sub-4B parameter language models over recent years, reflecting the increasing trend toward compact models optimized for edge and mobile deployment.

While these advancements improve feasibility for on-device inference, deploying even sub-10B models on edge devices remains computationally challenging. Unlike cloud environments, edge hardware is inherently constrained by limited memory, lower computational power, and energy efficiency concerns. Consequently, the trade-offs between model size, performance, and efficiency must be carefully evaluated to determine how well edge devices can handle LM inference in real-world applications.

To explore these trade-offs, this paper presents a comprehensive performance evaluation of generative LM inference on two distinct single-board computers (SBCs): the CPU-based Raspberry Pi 5 and the GPU-accelerated NVIDIA Jetson Orin Nano. Our study assesses key performance metrics, including memory usage, inference speed, and energy consumption, under different device configurations. Additionally, we investigate the throughput-energy trade-offs, cost implications, usability factors, and qualitative model performance. By quantifying the specific limits imposed by memory and energy constraints, this work wants to offer concrete and practical insights into the feasibility and trade-offs of running LMs at the edge.

Specifically, we explore the following research questions (RQ#):

- (RQ1) What are the computational limits of running LMs on edge devices?
- (RQ2) How do different model configurations (size, quantization) impact performance at the edge?
- (RQ3) What are the trade-offs between CPU- and GPU-based inference on resource-constrained hardware?
- (RQ4) How do system configurations (power modes, threading, etc.) affect inference efficiency, including microarchitectural-level performance metrics such as cache misses and context switches?
- (RQ5) What are the usability constraints, cost implications, and qualitative trade-offs when running LM inference on edge devices?

To address these questions, this work aims to provide a structured reference for understanding the performance trade-offs and practical limitations of LM inference on resource-constrained devices. Beyond offering insights for hardware-software co-design in edge AI, our findings contribute to a broader understanding of how edge devices can (or cannot) handle LM workloads effectively. This awareness is relevant for scenarios where distributed edge nodes must collaborate to execute LM inference, helping to inform the design of decentralized AI systems. Additionally, this study provides different insights for AI researchers optimizing

inference efficiency, system architects designing multi-node edge deployments, and industry practitioners integrating LMs into latency-sensitive IoT and 5G applications. The key contributions (C#) of this study are:

- (C1) Addressing (RQ1-3), we benchmark 11 generative LMs on two widely used SBCs, analyzing key performance indicators such as memory usage, inference speed, and energy efficiency to quantify the feasibility of edge inference.
- (C2) Answering (RQ2), we evaluate the effect of quantization and model scaling on inference efficiency, resource utilization, and model performance, highlighting the trade-offs between accuracy and computational cost.
- (C3) Directly addressing (RQ3), we compare CPU-based inference against GPU acceleration, investigating their impact on execution speed, energy consumption, and practical deployment feasibility on edge devices.
- (C4) Responding to (RQ4), we analyze the impact of power modes, threading configurations, and system settings, while also evaluating micro-architectural metrics, such as cache misses and context switches, to uncover bottlenecks and efficiency gaps in edge-based LM execution.
- (C5) Informed by (RQ5), we assess the practical challenges of running LMs at the edge, including inference cost analysis, qualitative benchmarking of the models, and aspects such as usability related to real-world applicability, providing a broader perspective beyond raw performance metrics.

The remainder of this paper is structured as follows: Section 2 provides background information on enabling technologies such as transformers and inference engines. Section 3 presents a selection of closely related work. Section 4 details the experimental methodology, while Section 5 presents the empirical results. In Section 6, these results are further discussed and contextualized, leading to the final conclusions in Section 7.

2 Background

This section provides an overview of the key concepts relevant to our study. We first describe the architecture of LMs, including the transformer architecture, KV-cache utilization, and model compression techniques such as quantization. Then, we introduce inference backends commonly used to execute LM inference on edge devices, which play an important role in determining computational feasibility.

Transformer Architecture and Large Language Models. The transformer architecture [50] was a breakthrough discovery, and most state-of-the-art LMs are still based on it. Its success stems from the multi-head attention mechanism, which does not rely on convolutions or recurrences, unlike previously established architectures. The attention mechanism computes key, value, and query vectors, where the key and value vectors of each token can be cached in the key-value cache (KV-cache) and reused in subsequent forward passes. A token is the fundamental unit of text that language models process. Tokens can represent entire words, subwords, or even individual characters, depending on the tokenization method used. Tokenization is the process of dividing a given text into discrete units (tokens). The KV-cache stores key and value vectors for all tokens within the current context, where the context refers to the sequence of previous tokens that still influence the generation of the next token. The maximum number of tokens that can be stored in the context is referred to as the context size. Because of the KV-cache, the generation of the first token exhibits different

computational characteristics compared to subsequent tokens. As a result, generative transformer inference is typically divided into two phases: the *prefill phase*, also called initialization or prompt processing phase, and the *generation phase*.

In the prefill phase, the model calculates the key and value vectors for every input token and then stores them in the KV-cache. This process is computationally expensive, making the prefill phase compute-bound. Conversely, in the generation phase, these cached vectors are reused, eliminating the need for recomputation. As a result, this phase is memory-bound, as it involves frequent memory accesses. Without a KV-cache, the time complexity of the attention layer is quadratic with respect to sequence length, whereas utilizing a KV-cache reduces the complexity to linear.

The original transformer architecture follows an encoder-decoder approach [9], consisting of two independent neural networks interacting between each other. The encoder computes a variable-length sequence and encodes it into a fixed-length vector. The decoder then takes this vector as input and generates a variable-length sequence as output. In the context of language processing, these variable-length sequences correspond to *tokenized* text sequences. Over time, new model variants emerged, using only encoders or only decoders. Encoder-only models tend to perform better for tasks that require language understanding (e.g., sentiment analysis), but they cannot generate text independently. A notable set of encoder-only models belongs to the BERT-family [13]. Decoder-only models are typically well-suited for tasks involving text generation. Examples of this model class include GPT-4 [35] or Llama 3 [17].

Due to the sheer size of LMs, various model compression techniques have been proposed to improve efficiency, one of the most widely used being quantization. Quantization reduces the model size by lowering the precision of model parameters [16, 23, 52]. Some quantization techniques focus solely on quantizing model weights, such as GPTQ [16] and k-quants [25]. Other approaches, such as SmoothQuant [52], also quantize model activations, further reducing computational complexity. Quantization techniques can further be classified into *post-training* quantization and *quantization-aware training*. Post-training quantization (e.g., GPTQ, k-quants, SmoothQuant) applies quantization after a model has been fully trained. Quantization-aware training (e.g., BitNet [28, 51]) incorporates quantization during training, reducing quality loss. However, it requires training from scratch, making it computationally expensive and inapplicable to pre-trained models. Some post-training quantization techniques embed limited re-training rounds to mitigate quality loss. These are referred to as n-shot quantization, where n denotes the number of re-training iterations. For example, GPTQ is a 1-shot quantization technique, while 0-shot quantization techniques (e.g., certain k-quants) require no re-training at all.

Inference Backends for LMs. An inference backend is a software tool required to execute AI model inference on a device. Various backends support LM inference across different hardware architectures, enabling execution on both CPU- and GPU-based systems. One of the most widely used inference backends for LMs is `llama.cpp` [26], known for its broad hardware support and ability to run models on both CPUs and GPUs. This backend system was chosen for this work, because of its flexibility and compatibility with various LM architectures. Another popular backend is `MLC LLM` [46], which offers a similar range of hardware and model support as `llama.cpp`. Additionally, it supports various quantization schemes [25], making it well-suited for optimized on-device inference. `picollm` [49] is another alternative, providing wide hardware support but offering a more limited model selection compared to `MLC LLM` and `llama.cpp`. It supports quantization and claims that its X-bit quantization significantly outperforms GPTQ [16], which is one of the most widely

used post-training quantization techniques. For on-device inference, another backend is `TinyChat` [20], which supports Activation-aware Weight Quantization (AWQ) [23] and SmoothQuant [52]. However, it currently supports fewer models than `llama.cpp` or MLC LLM and does not yet enable inference on mobile devices. Finally, Google’s `MediaPipe LLM Inference API` [44] enables LM inference capabilities for mobile phones and web applications. However, it currently supports only a limited selection of models.

3 Related Work

Benchmarking the performance of deep neural network (DNN) models on devices is not a new topic, and several benchmark suites have been proposed over time, such as AI Benchmark [19], EmBench [5] and MLPerf [39]. Among these, MLPerf has emerged as an industry standard for quantifying device performance for DNN training and inference across different DNN tasks, such as image classification or text summarization.

Table 1. Comparison with closely related papers

		Present work	[21]	[30]	[22]	[14]	[40]
Device Types	SBC (CPU)	✓	×	✓	×	✓	✓
	SBC (GPU)	✓	✓	×	×	×	✓
	Mobile Phones	×	✓	×	✓	×	×
Metrics	Latency/Throughput	✓	✓	✓	✓	✓	✓
	Energy	✓	✓	×	×	×	✓
	Memory	✓	✓	✓	✓	✓	✓
	Micro-architectural Metrics	✓	×	×	×	✓	×
Model Architectures	encoder-only	×	×	×	×	×	✓
	decoder-only	✓	✓	✓	✓	✓	×
	encoder-decoder	✓	×	×	×	×	×
Discussion Points	Configurations	✓	(✓)	×	×	×	×
	Throughput-Energy Trade-off	✓	×	×	×	×	×
	Usability	✓	✓	×	×	×	×
	Cost Analysis	✓	×	×	×	×	×

Recent studies have investigated the performance of transformer-based LMs on edge devices. A comparative overview of these works is provided in Table 1. Sarkar et al. [40] analyzed the performance of BERT-family models [13] on multiple SBCs across various NLP tasks. Their work also examined the impact of pruning on performance and accuracy. In contrast, our study focuses on generative models rather than encoder-only architectures and employs quantization as the primary model compression technique. Other works that focus on generative transformer models include [22], which analyzes LM inference on mobile phones, differing from our focus on SBCs. [14], and [30], which evaluates LM inference on SBCs but lack energy consumption measurements and do not discuss usability considerations for LM deployment at the edge. The study most closely related to our work is MELTing Point [21], which also investigates LM inference feasibility on edge devices, analyzing computational performance and energy usage. However, their study primarily focuses on mobile phones and GPU-accelerated edge devices, whereas our work extends the analysis to CPU-based inference on SBCs. MELTing Point is also the only prior work that discusses usability in detail based on its results. Furthermore, none of these studies explores how inference and system parameters—such as thread count and CPU governor settings—affect performance metrics. MELTing Point partially addresses this aspect by comparing different power modes on NVIDIA Orin devices, but does not generalize it to broader SBC hardware. Additionally, our study is one of the few to evaluate micro-architectural performance metrics

(e.g., cache misses, context switches) in the context of LM inference on edge devices—the only other known work that considers this aspect is Dhar et al. [14]. Finally, our work stands out by providing an in-depth discussion of energy-throughput trade-offs across different configurations and conducting a monetary cost analysis based on energy consumption during LM inference at the edge—an aspect not explored in previous studies.

4 Methodology

Table 2. Hardware characteristics of evaluated devices

	Raspberry Pi 5	Jetson Orin Nano Developer Kit
CPU	Arm Cortex-A76 (4 cores)	Arm Cortex-A78AE (6 cores)
GPU	VideoCore VII	NVIDIA Ampere (1024 CUDA cores)
RAM	8 GB LPDDR4X RAM	8 GB of LPDDR5 RAM
Storage	128 GB SanDisk High Endurance MicroSD	128 GB SanDisk High Endurance MicroSD
OS	Raspberry Pi OS (Debian-based)	NVIDIA Jetson Linux 36.3 (Ubuntu-based)

As mentioned in Section 1, for this study, we evaluated two widely used SBCs: a Raspberry Pi 5 (abbr. *RPi 5*) [38] and an NVIDIA Jetson Orin Nano Developer Kit (abbr. *Orin*) [31, 32]. These devices were chosen as they represent widespread and accessible platforms for CPU- and GPU-based edge computing. We deliberately excluded earlier versions of these devices, such as the Raspberry Pi 4 or the original NVIDIA Jetson Nano, as they were either unable to execute many experiments due to out-of-memory failures, or they did not provide enough computational power to execute LM inference at satisfying speeds [14], making them impractical for real-world LM inference. Conversely, we did not consider significantly more powerful edge devices, such as the Jetson AGX Orin, because its power supply requirements (19V, 90W) and peak power draw (~60W) place it closer to server-class hardware rather than the class of energy-constrained, low-power SBCs targeted in this study [41]. With this choice, we wanted to ensure that our evaluation captures realistic trade-offs between CPU- and GPU-accelerated LM inference on practical edge hardware while remaining within the power and resource limitations typical of IoT and edge deployments.

A summary of the hardware characteristics of both devices is provided in Table 2. To prevent thermal throttling, the RPi 5 was equipped with a Joy-it RB-Heatsink5, as overheating was observed during initial experiments. On the RPi 5, inference was exclusively CPU-based, while on the Orin, we evaluated both CPU and GPU inference.

For each device, multiple configurations were tested to analyze the impact of system settings on LLM inference performance. For CPU-based inference, the number of threads was varied from a single thread up to the maximum number of available CPU cores on each device. Additionally, three different CPU frequency scaling governors were evaluated. The *powersave* governor forces the CPU to always run at its minimum frequency, reducing power draw at the cost of potential performance degradation. The *performance* governor keeps the CPU at its maximum frequency at all times, ensuring the highest possible computational throughput. Finally, the *ondemand* governor dynamically adjusts the CPU frequency based on current workload demands, balancing power efficiency and performance; this was the default setting on both devices. For GPU-based inference, the Orin was tested under two predefined power modes: *7W*, which operates within a lower power envelope and may introduce performance constraints, and *15W* mode, which allows higher power draw for improved GPU performance. Additionally, a third setup was evaluated, where both

the CPU and GPU frequencies were set to their maximum limits within *15W* mode. This configuration, referred to as *MAX* mode, is used consistently throughout the remainder of this paper.

A single input prompt was used for evaluation, consisting of a summary task of a short story generated by ChatGPT. Due to differences in tokenization methods across models, the number of input tokens varied between 74 and 92, depending on the model. The number of output tokens was fixed at 100 to ensure consistency across experiments, allowing for controlled comparisons across models and configurations. To maintain comparability and repeatability, the context size was set to 512 tokens, as this was the lowest context size for which all evaluated models had been trained. These design choices were made to standardize the experimental setup while allowing fair performance comparisons across different models. While real-world applications may involve variable-length generations, evaluating inference performance across a fixed output length enables a systematic and reproducible assessment of computational trade-offs. Exploring how these trade-offs evolve at higher output scales remains an interesting direction for future work.

Table 3. Overview of evaluated models

Model name	Parameters (B)	Architecture	Abbreviation	Reference
Qwen 2 0.5B	0.5	decoder-only	Q2-0.5B	[53]
Flan T5 Large	0.8	encoder-decoder	FT5-L	[10]
Llama 3.2 1B	1.2	decoder-only	L3.2-1B	[4]
Qwen 2 0.5B	1.5	decoder-only	Q2-1.5B	[53]
Gemma 2 2B	2.6	decoder-only	G2-2B	[45]
Llama 3.2 3B	3.2	decoder-only	L3.2-3B	[4]
Phi 3.5 mini	3.8	decoder-only	P3.5-M	[1]
Yi 1.5 6B	6.1	decoder-only	Y1.5-6B	[3]
InterLM 2.5 7B	7.7	decoder-only	I2.5-7B	[8]
Llama 3.1 8B	8.0	decoder-only	L3.1-8B	[17]
Gemma 2 9B	9.2	decoder-only	G2-9B	[45]

The LMs under evaluation were selected based on their rankings in the Hugging Face Open LLM Leaderboard 2 [18]. To ensure a representative selection, we chose the highest-ranked model for each 1-billion-parameter range up to 9 billion parameters. Instruction fine-tuned base models were prioritized, even in cases where task-specific fine-tuned models ranked higher on the leaderboard. Models in the 4–6 billion parameter range were excluded from evaluation, as the only available models in this range were significantly lower ranked than several smaller models, making their inclusion less meaningful for comparative analysis. For models in the 0–1 billion parameter range, we evaluated two models due to differences in architecture. The highest-ranked model, Flan T5 Large, follows an encoder-decoder architecture, whereas all other evaluated models use a decoder-only architecture. To enable a fair comparison of architectural differences at a similar model scale, we also included the second-highest-ranked model, Qwen 0.5B. Additionally, we evaluated Llama 3.2 1B and 3B [4], which were released during the course of this study. Meta claims that these models have been optimized for Arm processors [4], making them particularly relevant for our evaluation. For each model, we tested two quantization schemes, Q_4_0 and $Q_4_K_M$ [25]. These schemes were chosen based on prior research, which has demonstrated that quantizing below 4 bits in blocking-based post-training quantization results in a significant drop in model quality [11, 21]. The models were quantized using the llama-quantize tool from llama.cpp. An overview of all evaluated models is provided in Table 3, which also includes abbreviations for model names that will be used in some figures throughout the paper for space efficiency.

All experiments were conducted using llama.cpp [26] (version 4501) as the inference engine. The experimental workflow was automated through a Bash script to ensure consistency across runs. For each evaluated model and configuration, five runs were performed to enhance statistical reliability. To maintain repeatability, all memory caches and swap memory were cleared before the first run of each experiment. Additionally, a 30-second pause was introduced between runs to allow the devices to cool down, preventing thermal effects from impacting results. To further ensure consistent thermal conditions, the fans on both devices were set to full speed throughout the duration of the experiments.

To measure various performance metrics, we utilized *perf*, a built-in Linux kernel profiler, along with a custom C script that retrieved system metrics from sysfs files. Current and voltage measurements on the RPi 5 were obtained from the power management integrated circuit, using code adapted from the vgencmd tool [15]. While this approach is widely used for energy measurements in edge computing, existing studies highlight that its accuracy and reliability are lower than those obtained via external hardware-based power measurement solutions [42]. However, the same studies indicate that for SBCs embedding GPUs, discrepancies are relatively minor, with the most significant deviations observed for discrete GPUs, such as PCIe-based accelerators. Additionally, these works provide regression-based mapping models, which can be leveraged to estimate real power consumption more accurately. Despite its limitations, our approach reflects a realistic measurement methodology—particularly in high-scale edge deployments where connecting external power measurement tools is often impractical. Given that internal measurement utilities are likely to be the default choice in real-world scenarios, our findings remain applicable and can be easily adjusted if needed. Measurements were recorded every 10 ms using *perf*, while the custom script implemented a 10 ms sleep interval between measurements. However, due to differences in execution time, the effective measurement intervals varied. On the Orin, the observed measurement interval was typically 15–20 ms, whereas on the RPi 5, it was 30–35 ms, primarily due to the long execution time of current and voltage measurements. We also tested shorter sleep intervals, but these caused significant interference with llama.cpp, distorting the results. Thus, the chosen interval provided a balance between measurement accuracy and minimal impact on inference performance.

To assess model quality, we measured the perplexity metric on the WikiText-2 test dataset [29] using llama-perplexity, a utility included with llama.cpp for performing various benchmarks. Perplexity quantifies a model’s uncertainty in predicting the next token, where lower values indicate higher confidence and better predictive performance and one is the optimal achievable value. The Flan T5 Large model was excluded from the qualitative assessment due to compatibility issues with llama-perplexity. The benchmark was conducted with a context size of 512.

5 Results

This section presents the experimental results. As described earlier, five runs were conducted for each model and configuration, with only runs two to five reported, as the first run served as a warm-up phase. However, differences between the first run and subsequent runs were minimal, except during the load phase, where extended loading times were observed. This phase refers to llama.cpp initializing and loading the model, and its impact will be discussed in the relevant subsections. To compare how different configurations—such as thread count, CPU governor, and power mode—affect various performance metrics, we present detailed results for a single model. Phi 3.5 Mini was chosen as the representative model since it is closest to the

center of the evaluated parameter range and did not exhibit significant outlier behavior in any metric. While most models followed similar trends across configurations, substantial outliers are highlighted separately. Despite models being similarly affected by configuration changes, their absolute performance levels varied. These differences are analyzed by presenting results for all models under a single selected configuration: (i) CPU governor set to *ondemand* (default setting), (ii) Power mode 15W (default setting), and (iii) Thread count as maximum available, except for generation throughput and energy consumption, where the optimal thread count was used per model and device.

Using the maximum thread count caused significant performance degradation in the generation phase, particularly for Q_4_0 quantization. To address this, we leveraged llama.cpp’s capability to assign separate thread counts for the prefill and generation phases, optimizing inference efficiency without negatively impacting system performance. Unlike thread count, modifying CPU governors and power modes affects the entire system, so we opted to keep them at their default settings to maintain consistency across experiments.

5.1 Memory

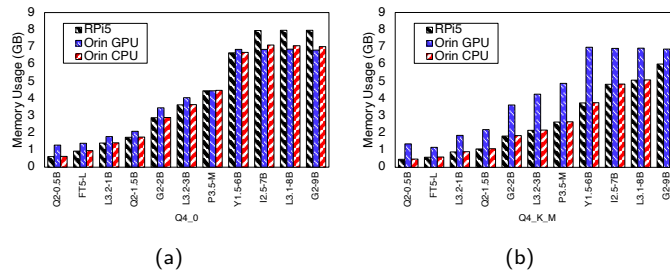


Fig. 3. Peak memory usage for all devices and quantization schemes

No significant differences in memory usage were observed across different system configurations. Therefore, this subsection focuses on model- and device-level comparisons.

As shown in Figure 3, CPU inference with $Q_4_K_M$ quantization exhibited an approximately linear relationship between peak memory usage and model size. This behavior is expected, as model weights account for most of the memory footprint. For GPU inference, a larger memory footprint was observed. This is primarily due to the shared main memory between the CPU and GPU on the Orin, leading to additional memory overhead. While the peak GPU memory usage was comparable to CPU inference, the CPU also allocated memory, further increasing overall memory consumption. This effect was particularly pronounced during the load phase, when the model was transferred to the GPU, as seen in Figure 4. During this phase, both GPU and CPU memory usage peaked simultaneously before the CPU memory allocation decreased, but still induced additional overhead. Another notable observation in GPU inference was the flattening of memory usage for models larger than Phi 3.5 Mini. This was due to the device exhausting its available memory. Despite having 8 GB of nominal memory, the usable memory was limited to below 7 GB, as the operating system and background processes collectively occupied over 1 GB.

In contrast, Q_4_0 quantization exhibited several notable differences in memory usage. First, GPU inference with Q_4_0 quantization resulted in a slightly lower peak memory footprint for most models,

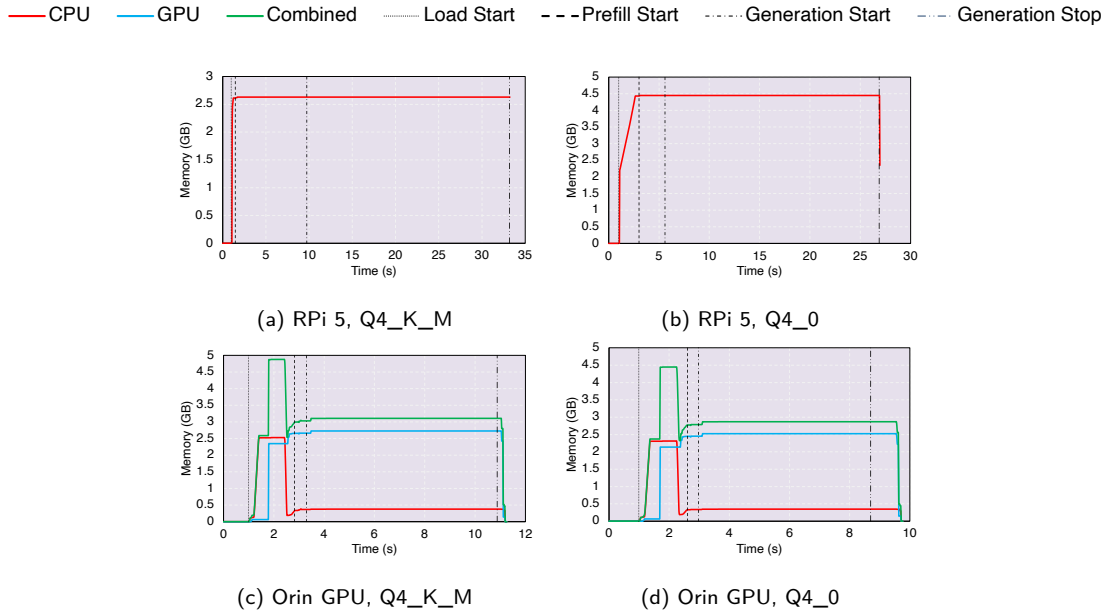


Fig. 4. Memory footprint timeline of one example run for RPi 5 (ondemand, 4 threads), Orin GPU (15 W) and both quantization schemes

whereas CPU inference showed a significantly higher memory footprint compared to $Q4_K_M$ quantization, as seen in Figure 3. The increased memory footprint for CPU inference may seem counterintuitive, as $Q4_0$ -quantized models are smaller than $Q4_K_M$ -quantized models. However, this behavior is likely due to the restructuring of model weights during the load phase to leverage optimized matrix multiplication kernels on the Arm CPU [27]. This restructuring process appears to require additional memory, which remains allocated throughout inference, as observed in Figure 4. This effect is not present in GPU inference, as model weights are not realigned when loaded onto the GPU. Despite this, for most models, GPU inference still had the highest memory footprint. However, for models larger than Yi 1.5 6B, CPU inference with $Q4_0$ quantization required more memory than GPU inference. Additionally, for Phi 3.5 Mini, memory usage was nearly identical between CPU and GPU inference. A second key observation is that the flattening of memory usage seen in GPU inference with $Q4_K_M$ quantization for larger models was also present in CPU inference with $Q4_0$ quantization. As before, this is due to memory exhaustion. The RPi 5's effective memory limit was higher than the Orin's, as its operating system consumed fewer memory resources. However, unlike with $Q4_K_M$ quantization, this memory saturation effect did not appear for Yi 1.5 6B under $Q4_0$ quantization.

It is worth noting that larger context sizes beyond 512 tokens were also tested. As the context size increases, the memory allocated for the KV-cache grows correspondingly. For extensive context sizes, the KV-cache memory footprint can even exceed the memory required for model weights. Even with a moderate context size of 1028, the largest model began to encounter performance issues. During CPU inference, constant page faults led to sharp performance declines. For GPU inference, the system experienced device crashes and

restarts. These findings highlight that memory is a critical bottleneck for use cases requiring larger models or extended context sizes, posing significant challenges for LLM inference on resource-constrained edge devices.

Main Takeaways

- Memory usage grows approximately linearly with model size
- GPU inference comes at the cost of significant memory overhead
- Q_4_0 quantization reduces memory footprint for GPU inference but adds substantial memory overhead for CPU inference compared to $Q_4_{K_M}$ quantization
- Memory is a main bottleneck for using very large models or context sizes on edge devices.

5.2 Inference Latency and Throughput

As shown in Figure 5, end-to-end latency generally decreases with an increasing thread count for both the RPi 5 and the Orin CPU under $Q_4_{K_M}$ quantization. However, with Q_4_0 quantization, the lowest latency was observed at two threads on the RPi 5 and four threads on the Orin CPU when using the *ondemand* and *performance* governors. This reduction was primarily due to a significantly shorter generation phase. Additionally, the *powersave* governor led to higher latencies compared to *ondemand* and *performance* governors. While no significant difference was observed between *ondemand* and *performance* on the RPi 5, the Orin CPU exhibited slightly lower latencies with the *performance* governor across most thread counts. An exception was observed with the *powersave* governor on the Orin, where the six-thread configuration resulted in a performance drop compared to five threads. This behavior was not observed on the RPi 5 but appears to be linked to a significantly higher number of context switches in this configuration, as illustrated in Figure 7. On the Orin GPU, the 15W power mode more than halves end-to-end latency compared to 7W mode, with maximum GPU frequency providing further minor latency improvements. When analyzing time to first token (TTFT)—the sum of load latency and prefill latency—distinct patterns emerge based on the quantization scheme. For $Q_4_{K_M}$ quantization, CPU inference is dominated by the prefill phase, which accounts for over 90% of TTFT across all configurations. In contrast, for GPU inference, the load phase is the bottleneck, making up 80% of TTFT. This is due to two factors: (i) the prefill phase is significantly shorter on the GPU than on the CPU, and (ii) the load phase takes 2–2.5 seconds on the GPU, compared to 1 second for CPU inference. For Q_4_0 quantization, the CPU inference load phase accounts for a significantly higher portion of TTFT (43%) in the fastest configuration. This is due to a substantial increase in loading time, which quadrupled in the worst case compared to $Q_4_{K_M}$ quantization, depending on the configuration. Additionally, Q_4_0 provides drastically lower prefill latencies, which were reduced by a factor of 3 to 4. For GPU inference, Q_4_0 quantization reduced both load and prefill latencies. However, the reported short load times are only valid for runs 2–5, as the model remains cached in memory between runs. In first-run scenarios, much higher load times were observed, ranging from 5 seconds to over 200 seconds, depending on the model size, quantization scheme, and device.

As shown in Figure 5, Q_4_0 quantization more than tripled prefill throughput and increased generation throughput by $\sim 10\text{--}70\%$ for CPU inference, compared to $Q_4_{K_M}$ quantization. This improvement aligns with expectations, as Q_4_0 quantization incorporates Arm processor optimizations applied during the load phase [27]. Interestingly, GPU inference also exhibited performance gains, with $\sim 30\%$ improvements in both the prefill and generation phases. For CPU inference, prefill phase throughput scales roughly linearly with increasing thread count, with *performance* and *ondemand* governors yielding higher throughputs than the

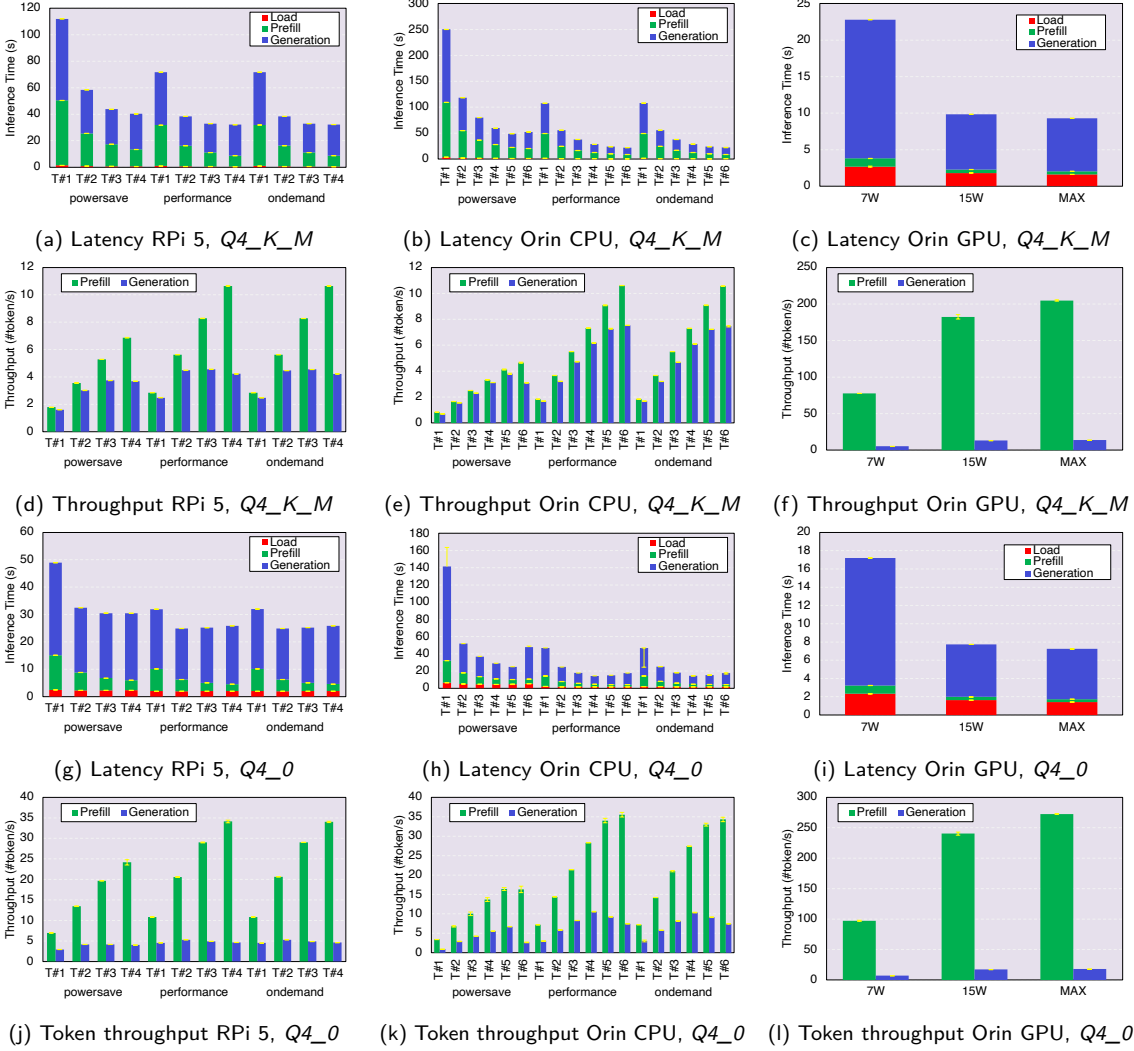


Fig. 5. Latency and throughput for multiple configurations, all quantization schemes and all devices

powersave governor. Similarly, generation throughput also increases linearly with thread count but eventually plateaus. On the Orin, plateaueing occurs at 6 threads while, on the RPi 5, plateaueing occurs at 3 or 4 threads with $Q4_K_M$ quantization, depending on the CPU governor. This behavior was observed for all models except Flan T5 Large, which did not exhibit a clear performance plateau. For the *powersave* governor, 3 threads yielded the highest throughput, while for *performance* and *ondemand* governors, 2 and 3 threads performed similarly. With $Q4_0$ quantization, 2 and 3 threads also performed similarly under *powersave*, whereas 2 threads provided the highest throughput for the other two governors. On the Orin CPU with $Q4_0$ quantization, a decline in prefill throughput was observed at 6 threads, while generation throughput peaked at 4 or 5 threads, depending on the model, before decreasing at higher thread counts under the

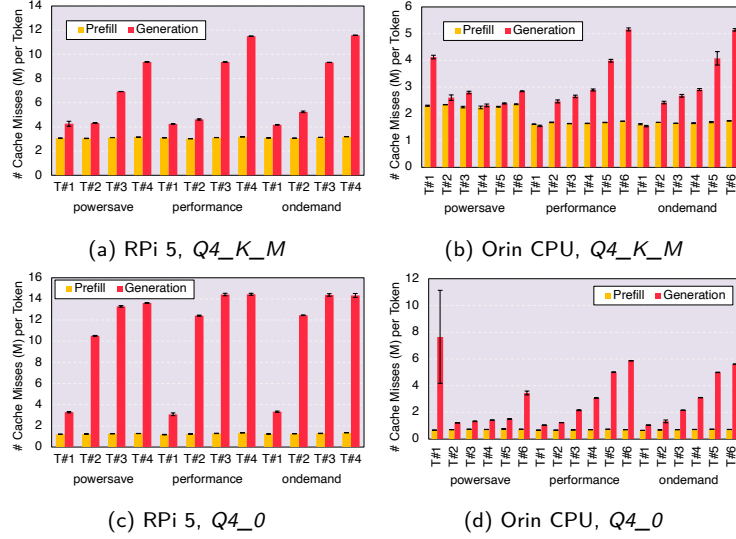


Fig. 6. Cache misses for multiple configuration, all quantization schemes, RPi 5, and Orin CPU

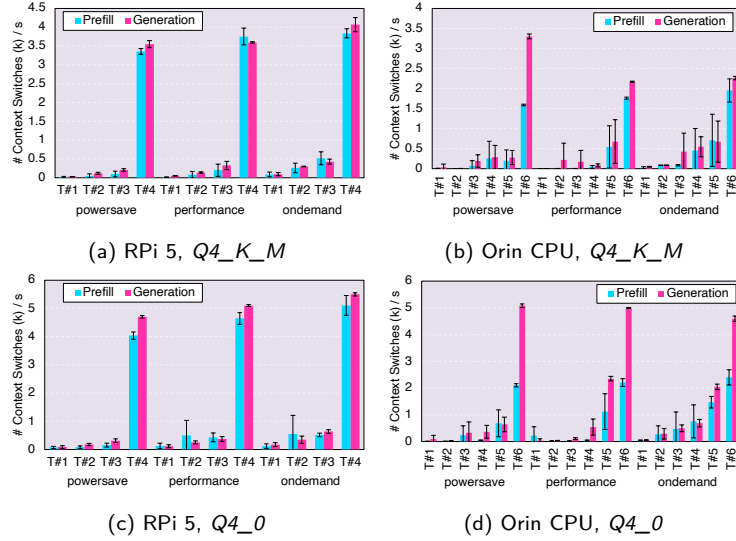


Fig. 7. Context switches for multiple configuration, all quantization schemes, RPi 5, and Orin CPU

performance and *ondemand* governors. For the *powersave* governor, 5 threads provided the best generation throughput. The decline in generation performance at higher thread counts is likely due to the generation phase being memory-bound, where performance is primarily constrained by memory access latency rather than computational power [36]. As a result, increasing compute resources beyond a certain point has only minimal impact on throughput. This effect becomes evident when examining level one (L1) cache misses per token in Figure 6. An increase in cache misses results in more frequent accesses to higher-level caches

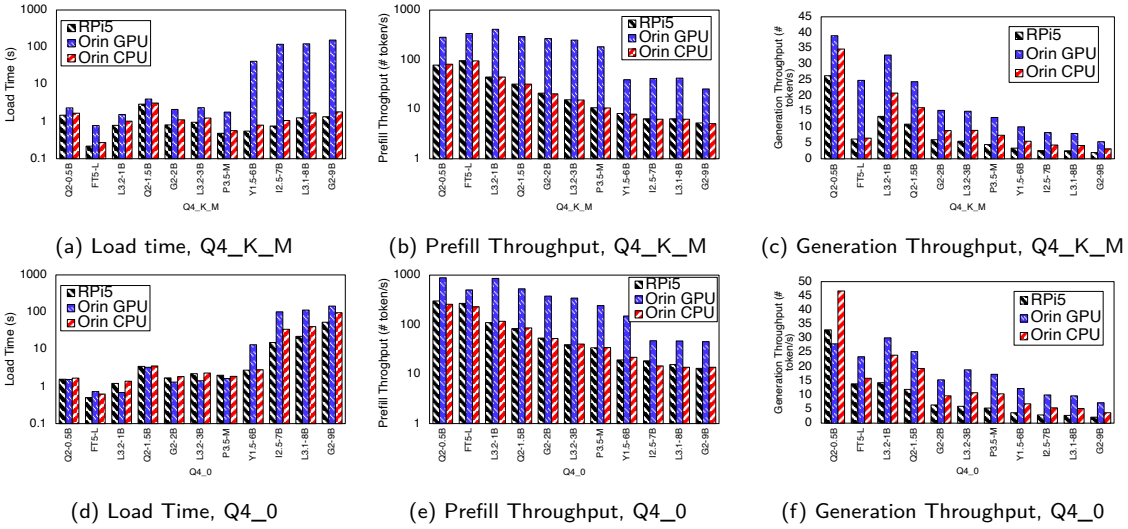


Fig. 8. Load time and throughput for all models, quantization schemes, and all devices

or even main memory, which are significantly slower than L1 cache and consequently lead to performance degradation. Additionally, an explosive increase in context switches was observed when using the maximum thread count on both devices. This is likely due to background processes competing for CPU time, displacing llama.cpp processes from the CPU. During the prefill phase, this effect is relatively minor, with only a slightly decreasing slope in token throughput. However, during the generation phase, throughput is significantly impacted due to the combined effect of elevated cache misses and excessive context switches. On the Orin with the *powersave* governor, a notable drop in generation throughput at six threads is apparent in Figure 5. This decline was not observed with the other governors and is likely due to higher context switch rates, which were approximately 50% higher than those seen with *ondemand* and *performance* governors.

For GPU inference, the *15W* power mode improves both prefill and generation throughput by a factor of ~ 2.5 compared to *7W* mode. Using maximum GPU frequencies further enhances prefill throughput by $\sim 12 - 13\%$, while the impact on generation throughput is less pronounced, with $\sim 4 - 5\%$ improvements.

Looking at Figure 8, it is evident that load time is higher for GPU inference with $Q4_K_M$ quantization. However, with $Q4_0$ quantization, GPU load time is shorter for most models up to Phi 3.5 Mini, as CPU loading times increase by factors ranging from $\sim 1.05\times$ for Qwen 2 0.5B to $\sim 4\times$ for Phi 3.5 Mini. For larger models, such as Yi 1.5 6B and beyond, load times increase dramatically, with factors between $\sim 17\times$ and $\sim 53\times$ compared to $Q4_K_M$ quantization. This occurs because the high memory footprint forces models to be evicted from memory during runs, requiring them to be reloaded from storage for each inference, significantly degrading performance. Additionally, a higher number of page faults was observed for these larger models, further increasing load times due to the slow nature of storage accesses. For $Q4_K_M$ quantization, this issue was only noticeable in GPU inference. However, for $Q4_0$ quantization, it also affected CPU inference, which can be explained by the increased memory footprint, as discussed in Subsection 5.1.

Figure 8 reveals that GPU inference consistently delivers the highest prefill throughput across all models and quantization schemes. In contrast, CPU inference shows comparable performance between the RPi 5 and Orin, except for Qwen 2 0.5B and Flan T5 Large under $Q4_0$ quantization, where the RPi 5 achieves noticeably better results. A general trend of decreasing prefill throughput with increasing model size can be observed. However, Llama 3.2 1B stands out as an exception, significantly exceeding expectations in GPU inference despite its relatively small size. Interestingly, this advantage was not present in CPU inference, contradicting Meta’s claim that Llama 3.2 models are optimized for Arm processors. Additionally, the largest models suffer a sharp drop in prefill performance, a consequence of their high memory footprint, as discussed earlier.

GPU inference achieves the highest generation throughput across all models, except for Qwen 2 0.5B under $Q4_0$ quantization. However, the performance gap between CPU and GPU inference is much smaller than in the prefill phase. This can be attributed to the memory-bound nature of the generation phase, where increased computational power has less impact on performance improvements. For CPU inference, the Orin significantly outperforms the RPi 5, with throughput gains of 32 – 67% for $Q4_K_M$ quantization and ~ 43 – 94% for $Q4_0$ quantization, depending on the model. However, for Flan T5 Large, this advantage is much less pronounced, with only $\sim 5\%$ and $\sim 14\%$ increases, respectively. This behavior is likely due to the Orin’s larger cache size, which reduces cache misses, as seen in Figure 6. When comparing model performance, the general trend of decreasing throughput with increasing model size remains evident. Notable exceptions include Flan T5 Large and Gemma 2 models, which underperform relative to their size expectations. Unlike in the prefill phase, no major performance drops were observed for the largest models during generation.

Main Takeaways

- GPU inference outperforms CPU inference in terms of token throughput at the cost of higher load times
- $Q4_0$ quantization substantially improves token throughput for all devices but induces higher load times for CPU inference compared to $Q4_K_M$ quantization
- Token throughput follows approximately a hyperbolic relationship with model size

5.3 Energy

In this subsection, we analyze the energy efficiency of LM inference across different configurations. Energy consumption is a critical factor in edge systems, particularly for battery-powered devices, where optimizing power usage directly impacts device longevity and real-world feasibility. Figure 9 illustrates the energy consumption per token for the Phi 3.5 Mini model across all tested configurations and devices. In most cases, the fastest configurations also exhibit the lowest energy consumption per token for both prefill and generation phases, as the reduction in inference time outweighs the increased power draw. However, some notable exceptions were observed. On the RPi 5, the *powersave* governor resulted in lower energy consumption per token than the *ondemand* and *performance* governors due to its reduced power draw, despite the longer inference time. On the Orin GPU, the *15W* mode consumed less energy per token than the *MAX* mode, as the power savings compensated for the higher inference time. Among all evaluated models, Qwen 2 0.5B and Llama 3.2 1B under $Q4_0$ quantization were the only exceptions, where the *MAX* mode achieved the lowest energy consumption per token during the generation phase on the Orin GPU. For all other models, energy consumption per token was approximately equal between *15W* and *MAX* mode, or *15W* performed slightly better, depending on the model. On the RPi 5, the optimal configuration in the prefill phase was

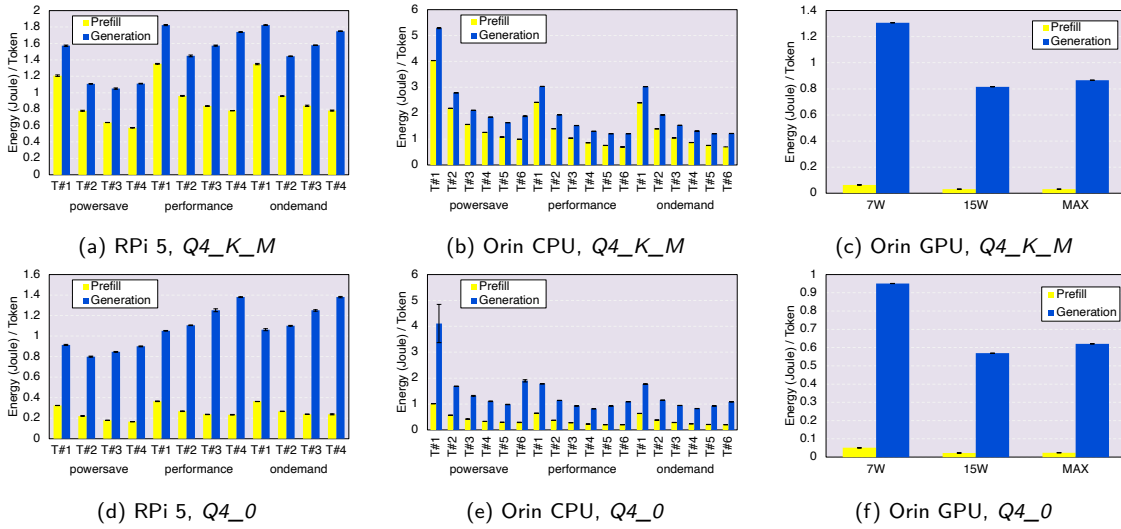


Fig. 9. Energy consumption per token for all configurations, quantization schemes, and devices

4 threads across all models, governors, and quantization schemes. However, in the generation phase, the optimal configuration varied depending on the model and quantization scheme. Flan T5 Large was a clear outlier, where 4 threads minimized energy consumption for all governors and quantization schemes, except for the *performance* governor with $Q4_0$ quantization, where 3 threads were more energy-efficient. For all other models, under $Q4_K_M$ quantization, 2 threads provided the best energy efficiency for both the *performance* and *ondemand* governors, while the *powersave* governor performed best with 3 threads. In the case of $Q4_0$ quantization, 2 threads were optimal for all models under the *powersave* governor, as well as for all models up to Llama 3.2 3B with the other two governors. For larger models, 1 thread resulted in the lowest energy consumption per token. On the Orin CPU, the *powersave* governor generally exhibited higher energy consumption compared to the *performance* and *ondemand* governors, which showed no significant differences in energy usage. In the prefill phase, the maximum thread count of 6 proved to be optimal across all models, governors, and quantization schemes. For the generation phase, under $Q4_K_M$ quantization, 5 threads yielded the best energy efficiency across all models and governors, except for Flan T5 Large with the *performance* and *powersave* governors, where 6 threads resulted in minimal energy consumption per token. When considering the $Q4_0$ quantization, 4 threads were optimal for the *performance* and *ondemand* governors, while 5 threads were best for the *powersave* governor across all models. The only exception was Flan T5 Large, which also showed optimal energy consumption with 5 threads under the *performance* and *ondemand* governors.

A comparison of quantization schemes reveals that $Q4_0$ quantization significantly reduces energy consumption. In the prefill phase, energy usage is lowered by factors of ~ 3 to ~ 4 for CPU inference. In the generation phase, CPU energy consumption decreases by $\sim 10\sim 70\%$, depending on the device and configuration. For GPU inference, energy consumption is reduced by $\sim 20\sim 40\%$. This reduction is

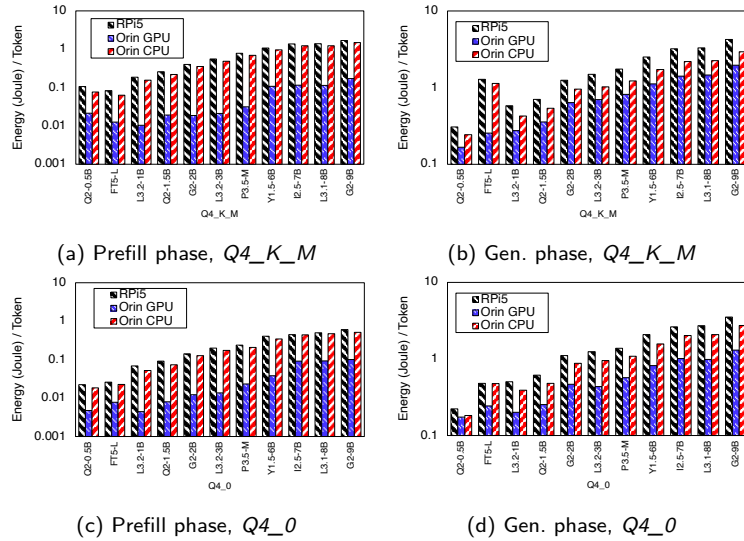


Fig. 10. Energy per token for all models, quantization schemes, and all devices

not solely due to increased inference speed but also to a moderate decrease in power draw compared to $Q4_K_M$ quantization.

When examining model-specific energy consumption in Figure 10, a general trend of increasing energy usage with model size is evident. This is primarily driven by longer inference latencies, although a slight increase in power draw is also observed. However, for Phi 3.5 and all larger models, average power draw remained approximately constant. In the generation phase, Flan T5 Large emerged as a notable outlier, exhibiting substantially higher energy consumption relative to its size. This inefficiency stems from its lower generation speed, leading to longer active power draw.

For all models, GPU inference significantly reduced energy consumption compared to the RPi 5, with improvements by factors of $\sim 3.3\sim 26.4$ in the prefill phase and $\sim 1.2\sim 5.0$ in the generation phase, depending on the model and quantization scheme. For CPU inference, the Orin also demonstrated superior energy efficiency over the RPi 5 in both phases. In the prefill phase, this improvement was primarily due to a lower mean power draw, resulting in energy reductions of $\sim 12.0\sim 38.7\%$ for $Q4_K_M$ quantization and $\sim 1.8\sim 32.3\%$ for $Q4_0$ quantization. In the generation phase, the lower inference latencies on the Orin further amplified this difference, leading to energy consumption reductions of $\sim 22.2\sim 47.2\%$. Flan T5 Large was the only model with a significantly smaller energy efficiency improvement, showing just $\sim 13\%$ for $Q4_K_M$ quantization and $\sim 0.9\%$ for $Q4_0$ quantization. $Q4_0$ quantization consistently outperformed $Q4_K_M$ quantization in terms of energy efficiency for almost all models and devices, mainly due to reduced inference time but also because of a slightly lower power draw. In the prefill phase, the efficiency improvement factors ranged between ~ 1.2 and ~ 4.7 , depending on the model and device. In the generation phase, improvements were ~ 1.04 to ~ 2.7 , with one notable exception: Qwen 2 0.5B in GPU inference, where energy consumption increased by $\sim 5\%$ compared to $Q4_K_M$ quantization.

Main Takeaways

- GPU inference is more energy efficient than CPU inference in both prefill and generation phase
- Q_4_0 quantization improves energy efficiency on all devices for both prefill and generation phase over $Q_4_K_M$ quantization

5.4 Quantization Effect

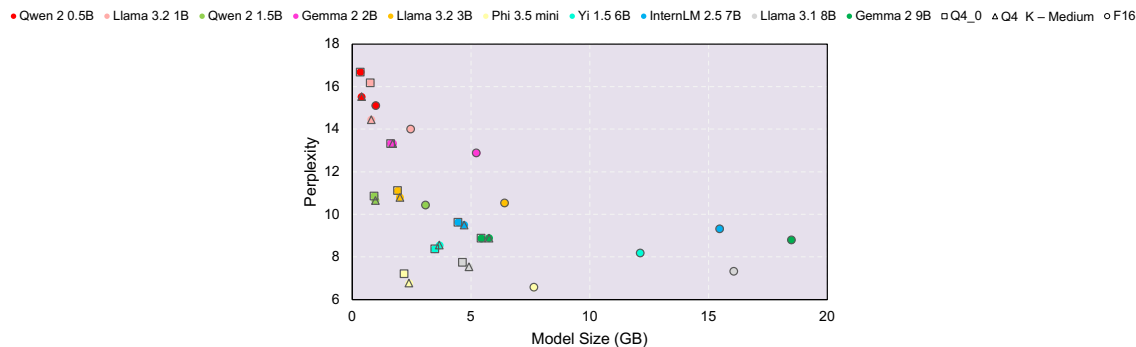


Fig. 11. Results of qualitative benchmarks

Since quantized models were used in this evaluation, it is essential to assess how quantization impacts both output quality and computational performance compared to unquantized models. To analyze the effects on output quality, a perplexity benchmark was conducted, with results presented in Figure 11. The findings reveal a perplexity increase across both quantization schemes and all models when compared to their 16-bit floating point counterparts. This effect was particularly pronounced for the smallest models. Additionally, a clear distinction between quantization schemes emerged: Q_4_0 quantization exhibited higher perplexity than $Q_4_K_M$ quantization for all models, except for Yi 1.5 6B and the Gemma models, where both schemes performed similarly. Beyond perplexity, a set of commonsense reasoning and question-answering benchmarks was conducted. Overall, no significant accuracy drops were observed across these tasks. However, detailed results are omitted for space reasons, as previous studies have identified perplexity as a more robust metric for quantifying the impact of quantization [12]. For a broader perspective, we refer to Laskaridis et al. [21], who performed the same set of benchmarks and reported similar results, despite evaluating a different set of models.

To evaluate the impact of quantization on computational performance, Figures 12 illustrate how quantization affected memory footprint, token throughput, and energy consumption for all models that were small enough to fit their full-precision versions into memory. In terms of memory footprint reduction, as shown in Figure 12, quantization significantly reduces memory usage, with reductions by factors between 1.7 and 3 across all models, devices, and quantization schemes. However, as previously discussed, Q_4_0 quantization exhibits a higher memory footprint for CPU inference but a lower footprint for GPU inference compared to $Q_4_K_M$ quantization. Analyzing the effects on token Throughput and energy consumption, $Q_4_K_M$ quantization negatively impacted both token throughput and energy consumption in the prefill phase, with varying intensity depending on the model and device. Throughput reductions ranged between

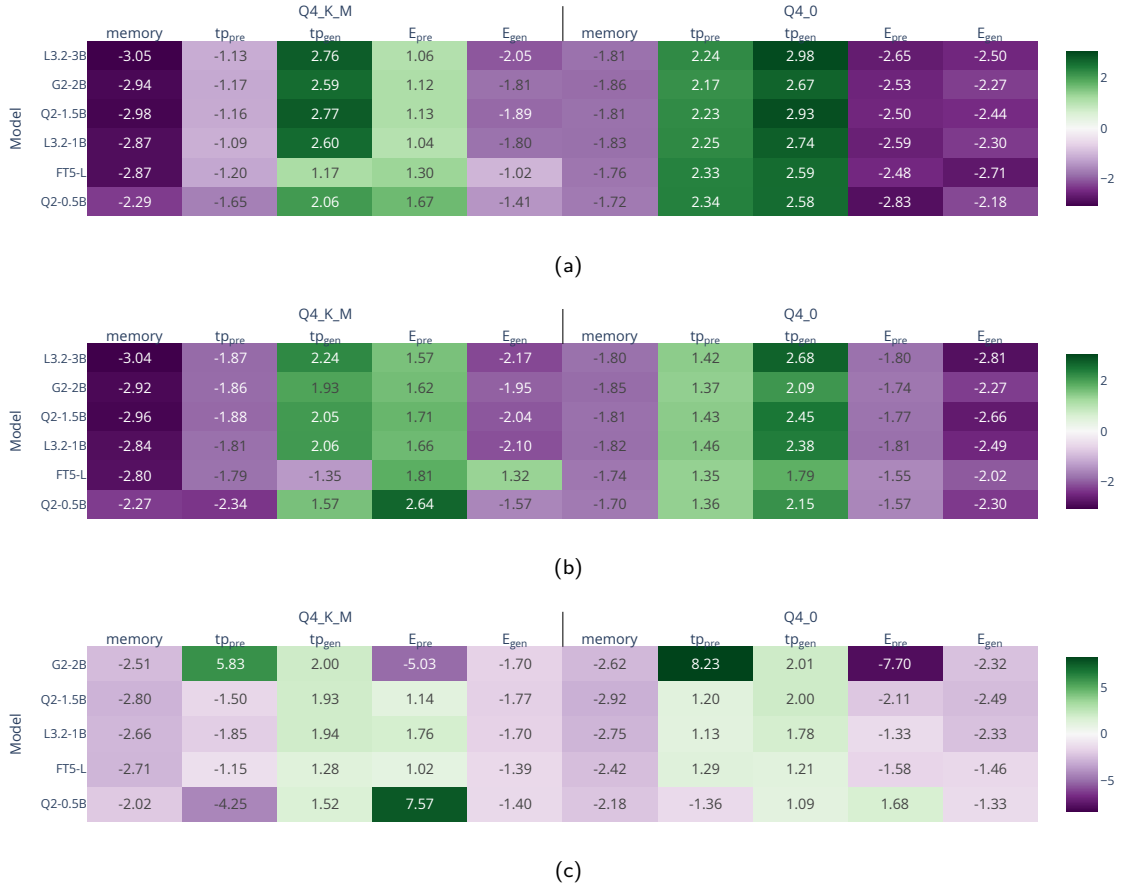


Fig. 12. Change factors on various metrics on RPi 5 (a), Orin CPU (b), and Orin GPU (c) compared to 16 bit floating point models. Negative numbers indicate decrease by absolute value.

factors of 1.09 and 4.25, while energy consumption increased by factors between 1.04 and 7.57. Conversely, in the generation phase, $Q4_K_M$ quantization led to performance improvements, where token throughput increased by factors between 1.17 and 2.76, and energy consumption decreased by factors ranging from 1.02 to 2.17. When it comes to outliers, Gemma 2 2B exhibited unexpected improvements in both prefill throughput and energy consumption for GPU inference. Flan T5 Large showed degraded performance in generation throughput and energy consumption on the Orin CPU. In contrast, $Q4_0$ quantization yielded consistent improvements in both throughput and energy consumption across both phases, with the only exception being Qwen 2 0.5B, which exhibited a performance drop in the prefill phase for GPU inference. The improved performance in the generation phase can be attributed to the memory-bound nature of this phase. Since quantized model weights require lower precision, a greater portion of them fits into cache, leading to fewer cache misses and ultimately faster token generation.

Main Takeaways

- In terms of perplexity, $Q4_K_M$ quantization performed better than $Q4_0$ quantization for most models, especially for the smallest evaluated models. Overall, perplexity increases was especially pronounced for the smallest models.
- $Q4_0$ quantization improves all memory footprint, token throughput, and energy consumption compared to full-precision models, while $Q4_K_M$ quantization resulted in inferior throughput and energy consumption in the prefill phase.

6 Analysis and Trade-Offs Discussion

Optimizing LM inference at the edge requires balancing multiple constraints, including computational performance, energy efficiency, and cost. In this section, we leverage our empirical measurements to analyze key trade-offs, assess its practical usability in real-world deployments, and evaluate the economic feasibility of LM inference on edge devices.

6.1 Throughput-Energy Trade-Off

On the Orin CPU, the fastest configuration was either also the most energy-efficient or, at worst, only marginally less efficient than the optimal configuration. However, no single configuration simultaneously maximized performance and energy efficiency on the RPi 5 or the Orin GPU. To determine the optimal trade-off between token throughput and energy consumption, we define the metric action per token S_t as the ratio between the energy E consumed during an inference phase and the token throughput t :

$$S_t = \frac{E}{t}$$

This metric represents the amount of action required to process a token during the prefill phase or generate a token in the generation phase. A lower action per token value indicates higher efficiency and is therefore considered preferable in our analysis. The term *action* is used because the resulting unit, $\frac{\text{joule-seconds}}{\text{token}}$, corresponds to the physical unit of action in physics. Additionally, the symbol S was chosen as it is commonly used to denote action in physics.

When calculating S_t for the prefill phase, Figures 13 show that the *ondemand* and *performance* governors achieved a 10–18% lower action per token compared to the *powersave* governor for $Q4_K_M$ quantization. In contrast, no significant differences were observed between governors for $Q4_0$ quantization, with the optimal governor varying depending on the model. Only results for 4 threads are reported, as this configuration provided the best balance between energy consumption and token throughput across all models.

When analyzing the generation phase results in Figures 14, it is evident that for $Q4_K_M$ quantization, the *powersave* governor yielded the lowest action per token, with the only exception being Flan T5 Large, where the *performance* governor with 4 threads performed best. However, the optimal thread count varied by model. For most smaller models (up to Llama 3.2 3B), 3 threads provided the best efficiency while, for most larger models, 2 threads were optimal. There are still a few exceptions. First, Qwen 2 0.5B (despite its small size) performed best with 2 threads. Second, Gemma 2 9B (the largest model) performed best with 3 threads. Similarly, for $Q4_0$ quantization, the *powersave* governor with 2 threads resulted in optimal efficiency across all models except Flan T5 Large, where the *ondemand* governor with 4 threads performed best. Overall, these results suggest that for all decoder-only models, the *powersave* governor was the most

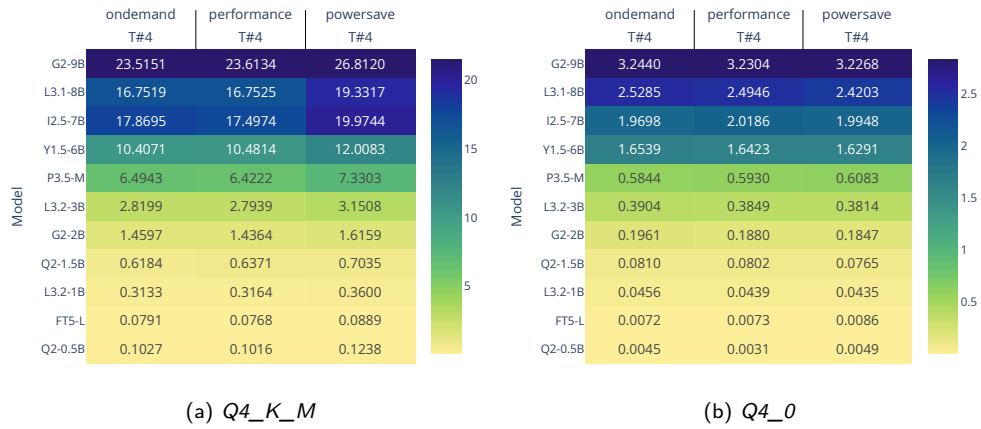


Fig. 13. Prefill action per token

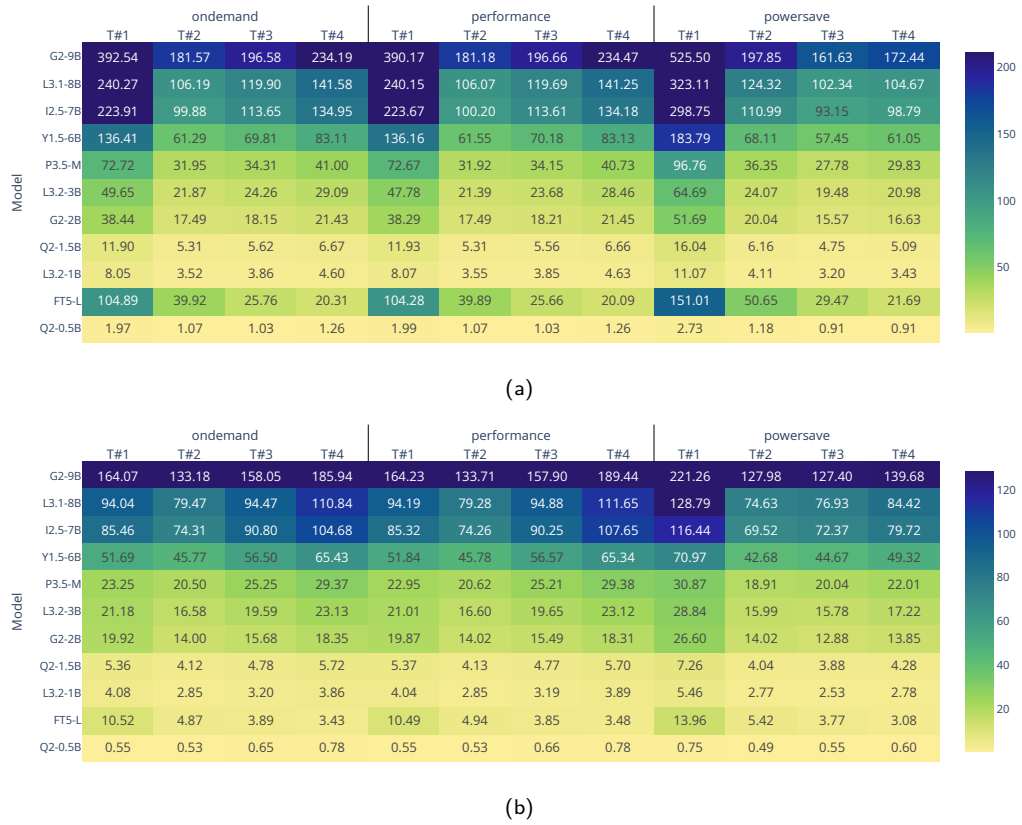


Fig. 14. Comparison of generation action per token for $Q4_K_M$ (a) and $Q4_0$ (b).

energy-efficient choice in both inference phases. However, the optimal thread count in the generation phase (for $Q_4_K_M$ quantization) varied by model size, suggesting a potential correlation between model size and ideal thread allocation.

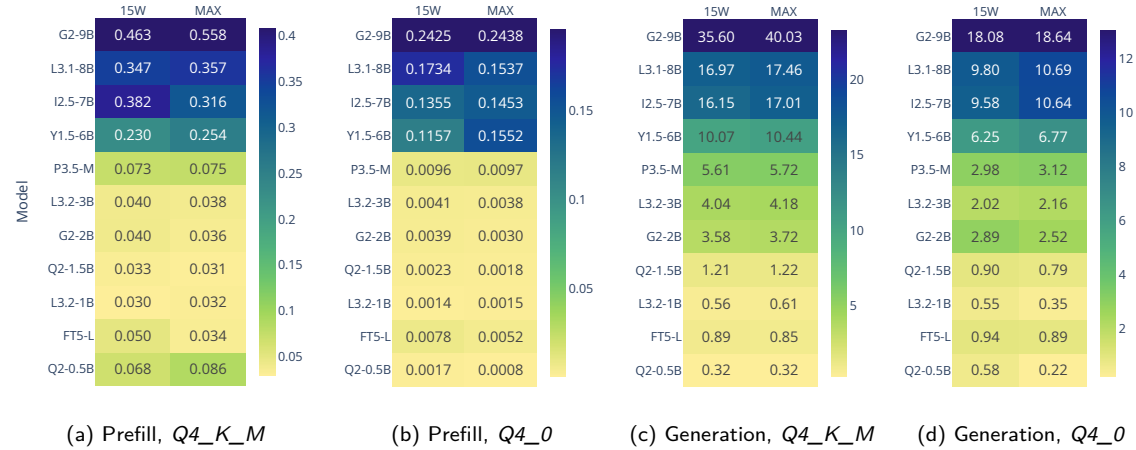


Fig. 15. Action per token for prefill and generation phase for all power modes on Orin GPU

On the Orin GPU, the $15W$ mode resulted in the lowest energy consumption across all models, while the MAX mode provided the highest inference speeds at the cost of increased energy usage. When using action per token as the decisive metric, it becomes evident that, for most models, the MAX mode offered the best energy-throughput trade-off in the prefill phase for both quantization schemes. However, there were, once again, some outliers. In fact, for both quantization schemes, Yi 1.5 6B and Gemma 2 9B achieved optimal efficiency with the $15W$ mode. Additionally, for $Q_4_K_M$ quantization, Qwen 2 0.5B and Llama 3.1 8B also performed best in the $15W$ mode.

In the generation phase, the MAX mode yielded the optimal trade-off for all models up to Qwen 2 1.5B with $Q_4_K_M$ quantization and up to Gemma 2 2B with Q_4_0 quantization. However, for larger models, the $15W$ mode proved to be more efficient. Results for the $7W$ mode were omitted, as it performed worse than the other two power modes in both token throughput and energy consumption.

Overall, a clear trend emerged: the MAX mode provided better performance for smaller models, whereas the $15W$ mode was more efficient for larger models.

Main Takeaways

- For the prefill phase on the RPi 5, the *ondemand* and *performance* CPU governors performed best with $Q_4_K_M$ quantization but for Q_4_0 quantization, no significant differences were observed and the optimal governor depended on the model.
- In the generation phase, the *powersave* governor with 2 threads for almost all models with Q_4_0 quantization and for most larger tested models with $Q_4_K_M$ quantization performed best, while 3 threads performed best for most of the smallest tested models with $Q_4_K_M$ quantization.

- For GPU inference the *MAX* mode showed the optimal throughput-energy trade-off for most models in the prefill phase
- The *MAX* mode performed best for most smaller models in the generation phase, while for most larger models the *15W* mode provided optimal action per token

6.2 Significance for Usability

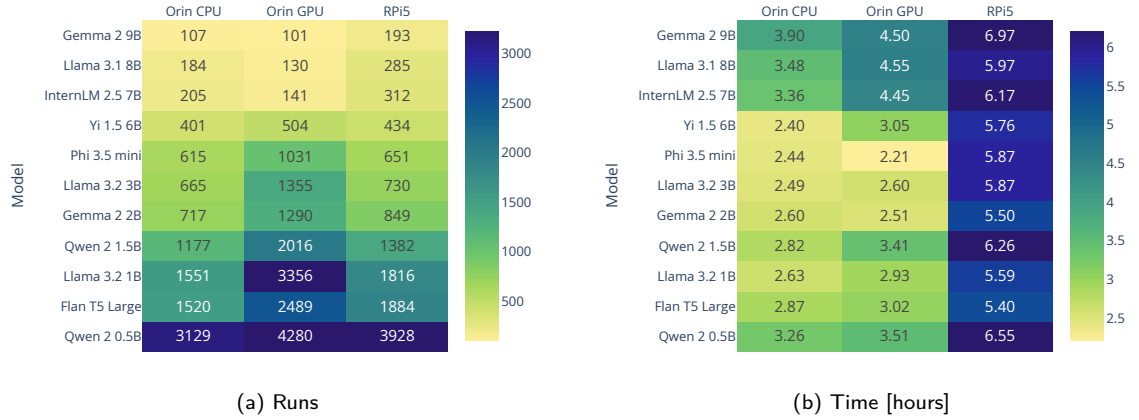


Fig. 16. Number of inference runs and Time [hours] until battery recharge for configurations with minimal energy consumption per run

In the following, we analyze how inference speed and energy consumption impact the usability of LMs in real-world systems.

One key challenge is the long load times observed during the first run of each experiment and for all runs of larger models on the Orin. In any interactive use case, where users expect real-time responses, these high loading times—which translate to significant latencies—would likely degrade the user experience. To mitigate this, it is crucial to keep the model in memory between runs, as this substantially reduces load times, as discussed in Section 5.

Another potential limitation is the high memory demand of the models, even when they fit within the device’s main memory. First, our results indicate that for the largest evaluated models, complications arose during GPU inference across both quantization schemes, as well as in CPU inference with Q_4_0 quantization, leading to significantly increased loading times and reduced prefill performance. Second, in real-world deployments, edge devices are often not dedicated solely to LM inference but may need to support additional applications. If the inference process occupies the majority of system memory, other applications may fail to run concurrently, leading to frequent memory paging. Since storage accesses are inherently time-consuming, this could cause substantial performance degradation.

For use cases where human users read generated tokens in real-time, reading speed serves as a baseline to determine whether token throughput is sufficient to maintain a smooth user experience. If tokens are generated slower than the average reading speed, users may need to pause frequently, leading to disruptions and a degraded experience [24]. The average reading speed of an English reader is approximately 4 words

per second [7]. According to OpenAI, one token corresponds to roughly 0.75 words [48]. Based on this, an optimal generation throughput should be at least $5.3 \frac{\text{tokens}}{\text{s}}$ to ensure a seamless experience. However, human reading speed varies significantly between individuals; therefore, this threshold should be considered only as an approximate guideline for assessing generation speed requirements in such use cases. When selecting the highest generation throughput for each model on the RPi 5, only models up to Llama 3.2 3B with $Q4_K_M$ quantization and up to Phi 3.5 mini with $Q4_0$ quantization were able to exceed the $5.3 \frac{\text{tokens}}{\text{s}}$ threshold. For Orin CPU inference, all models up to Yi 1.5 6B with $Q4_K_M$ quantization and up to InternLM 2.5 7B with $Q4_0$ quantization met this requirement. However, for larger models, a degraded user experience seems likely due to insufficient generation throughput. In contrast, on the Orin with GPU inference, all models exceeded $5.3 \frac{\text{tokens}}{\text{s}}$ for both quantization schemes, ensuring a smoother reading experience.

However, generation speed requirements depend on the specific use case. In some scenarios, lower generation speeds may be sufficient, while in others, higher speeds could be advantageous. For instance, if an LM is summarizing documents as a background process—without user interaction or strict time constraints—slower generation speeds may be acceptable. In contrast, multi-agent LM systems could benefit from higher generation speeds, as LMs can typically process input tokens much faster than human reading speed.

As edge devices are often battery-powered or have limited energy availability, it is important to assess how many inference runs can be performed before the device runs out of battery. For each model, we used the configuration with the lowest mean energy consumption per run (considering runs 2–5 of an experiment) to estimate the number of inference runs that could be executed at 100% utilization (i.e., with no idle time) on a fully charged smartphone battery. As a representative example, we selected the Samsung Galaxy S24 Ultra, a high-end smartphone with a nominal battery capacity of $18.84Wh = 67824J$. The longest run times were observed on the RPi 5, primarily due to its slower inference speed. However, even in this case, the maximum runtime remained below 7 hours, raising concerns about the feasibility of LM inference in energy-constrained environments, particularly when inference is performed frequently. That said, it is important to acknowledge the caveats of this analysis. First, our analysis considers only one input prompt, whereas different prompts could lead to variations in both the number of inference runs and total runtime before recharging. Second, as discussed earlier, our energy measurements likely underestimate actual consumption, as they do not account for all device peripherals or power supply inefficiencies. Third, the configurations minimizing total energy consumption were used for this evaluation. On the RPi 5, this often corresponds to the *powersave* governor, which reduces inference speed. In real-world applications, this performance might be too slow, necessitating a less energy-efficient configuration. Due to the second and third points, these results should be interpreted as an upper bound on the number of feasible inference runs.

Main Takeaways

- It is doubtful whether generation speed of edge in inference is satisfying for the largest evaluated models for a wide range of use cases, especially with CPU inference
- However, performance for smaller models is likely satisfactory for many uses cases as generation throughput exceeded average human read speed even with CPU inference
- Due to the high energy consumption, it is questionable whether highly frequent LM inference is feasible in energy-constrained environment

6.3 Cost Analysis

With self-deployed models at the edge, no service costs are incurred for the user in contrast to the API costs of cloud services. For instance, at the time of writing, executing inference with the *GPT-4o mini* model via the OpenAI API incurs a cost of 15¢ per million input tokens and 60¢ per million output tokens¹ [33].

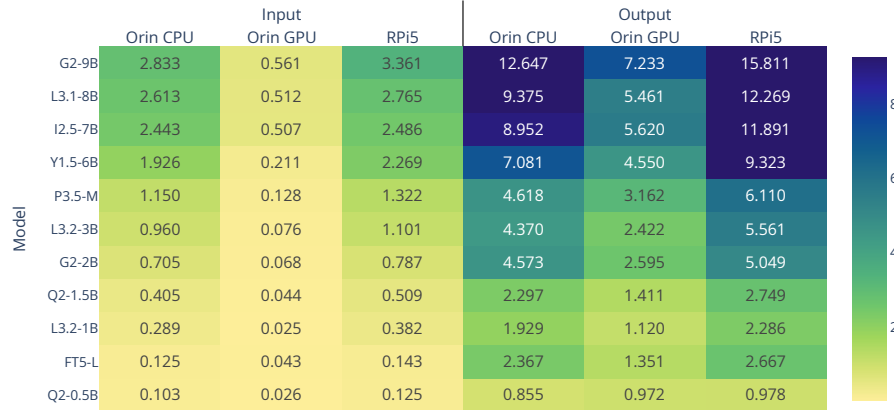


Fig. 17. Energy cost per one million input and output tokens for different devices in cents

However, edge deployments also incur operational costs, as energy consumption contributes to long-term expenses, in addition to the initial device purchase price. Using energy measurements from our experiments, we computed the cost per one million input and output tokens (illustrated in Figure 17). The calculations assume an optimal thread count with the *ondemand* governor for CPU inference, while for GPU inference, the *15W* power mode was selected as the most energy-efficient setting. An electricity price of 20¢/kWh was chosen as a middle ground, considering that energy costs vary significantly by location and sector. For example, in the U.S., electricity prices in September 2024 ranged from under 10¢/kWh to over 40¢/kWh [2].

It can further be observed that the operational costs for one million input tokens range from 0.025¢ for Llama 3.2 1B on GPU to 3.361¢ for Gemma 2 9B on the RPi 5. Even in the most expensive scenario, this remains 4.46 times cheaper than the service cost of the OpenAI API, while in the best-case scenario, it is 600 times lower. For one million output tokens, the energy costs span from 0.855¢ for Qwen 2 0.5B on the Orin CPU up to 15.811¢ for Gemma 2 9B on the RPi 5. Even in the worst-case scenario, the cost remains 3.79 times lower than the OpenAI API service cost for GPT-4o mini, while in the best-case scenario, it is 70.18 times lower.

However, several caveats should be considered when interpreting these cost estimates. First, as discussed in Section 4, our energy measurements likely underestimate actual energy consumption, as they exclude certain device components, such as USB ports, and do not account for power supply inefficiencies or energy usage during loading and idle states. Second, the operational costs presented here only consider energy consumption, whereas other expenses, such as device maintenance, may also contribute to the total cost.

¹"Ignoring Batch API prices and cached token prices"

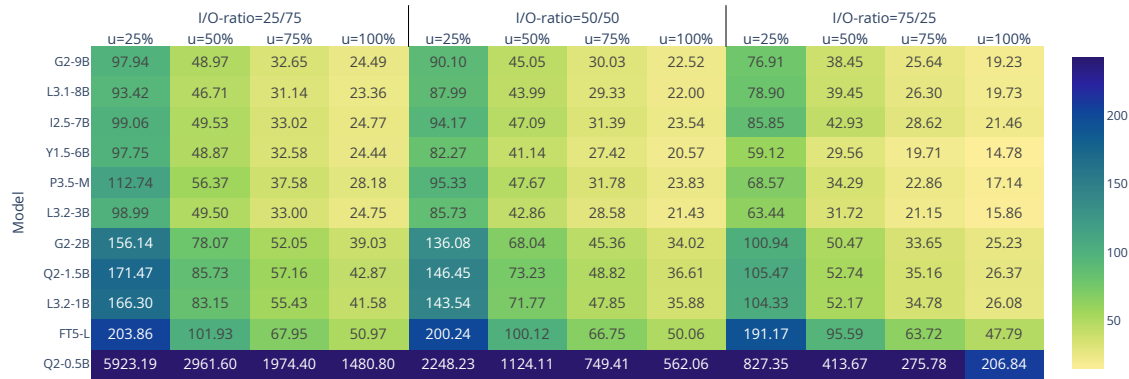


Fig. 18. Break-even time in years between RPi 5 and Orin GPU for different IO-token ratios and device utilizations.

Third, these estimates do not factor in model quality, meaning that higher cloud service prices may be justified by more sophisticated model capabilities. Thus, to derive definitive conclusions, more precise energy measurements and a more comprehensive cost model incorporating additional operational factors are required.

Despite these considerations, the significantly lower operational costs—particularly for smaller models on GPU—suggest that self-deploying LMs at the edge could be more cost-efficient than cloud services in certain scenarios. This is especially relevant when idle edge resources can be leveraged, as this eliminates device acquisition costs. Moreover, self-deployment allows greater flexibility in model selection, enabling the deployment of the smallest model that meets task-specific requirements. Given that smaller models consume substantially less energy, as demonstrated in our results, this approach could yield further cost benefits. However, in scenarios where highly sophisticated model capabilities are essential, cloud services may still be the more economical option.

Beyond comparing edge inference with cloud services, it is also valuable to analyze the cost differences between the tested devices. As shown in Figure 17, GPU inference on the Orin incurs significantly lower energy costs compared to CPU inference on the RPi 5. However, the initial device cost must also be considered. While the RPi 5 is much more affordable, the Orin’s higher efficiency raises the question of when its purchase becomes justifiable from a cost perspective. Based on retail prices from DigiKey’s US store at the time of writing, the RPi 5 (including power supply and fan) costs \$97, whereas the Orin is priced at \$598.80—resulting in a price difference of \$501.80.

To better understand the cost-effectiveness of choosing the Orin over the RPi 5, we calculated break-even times for 12 scenarios with varying input/output token ratios and device utilization (μ). The break-even time represents the duration needed for the operational cost savings of the Orin to offset its higher purchase price. For these calculations, we assumed an electricity price of 20¢/kWh. The RPi 5 was tested with the default governor (*ondemand*) and throughput-optimal thread counts, while the Orin used the default power mode (15W). Since $Q4_0$ quantization proved more energy-efficient across both inference phases, we based our comparison on its results, excluding the energy consumption of the loading phase. As shown in Figure

18, input-heavy workloads result in shorter break-even times compared to output-heavy workloads, as the energy savings of GPU inference are more pronounced in the prefill phase than in the generation phase. Even with $\mu = 100\%$ utilization (i.e., continuous inference with no idle time), the fastest break-even scenario takes nearly 15 years. For balanced or output-heavy workloads, the required time increases even further, making it unlikely that the Orin would ever financially break even in typical edge AI deployments.

While these break-even time estimates provide insight, several caveats must be considered when interpreting the results. First, our energy measurements exclude certain board components on both devices, which may slightly affect the absolute energy consumption values but should not significantly alter the comparative results, as similar components are omitted for both the RPi 5 and Orin. Second, electricity prices have a direct inverse impact on break-even times. Doubling the electricity price would halve the time required to offset the Orin’s higher purchase cost. Third, computational performance is not accounted for in this analysis. In this respect, the higher throughput of the Orin may justify its higher purchase price for certain computationally demanding use cases. The utilization values in Figure 18 are based on the Orin, which is the more powerful device. As a result, in some scenarios, the RPi 5 would require utilization exceeding 100% to match the Orin’s performance, which is not feasible. Consequently, the break-even times for workloads corresponding to $\mu = 100\%$ on the RPi 5 are significantly longer than the minimum values observed. Thus, for workloads where the RPi 5 provides sufficient performance, it remains the more cost-effective choice over the Orin.

Main Takeaways

- Edge inference could potentially yield cost benefits over cloud services due to its flexibility in model choice
- From a pure cost perspective the RPi 5 is the more efficient device than the Orin

7 Conclusions

In this paper, we explored the feasibility and trade-offs of LM inference on edge devices, evaluating key performance factors such as memory usage, inference speed, and energy consumption across CPU- and GPU-based platforms. Our findings highlight the complex interplay between model size, hardware constraints, and quantization strategies, emphasizing the need for careful optimization to enable practical deployment in edge environments. While challenges remain with the current state-of-the-art technologies, our results also reveal promising opportunities, particularly in specific usability scenarios where local inference enhances responsiveness and autonomy, as well as potential cost benefits over cloud-based alternatives. We are confident that this study can contribute to advancing the R&D landscape of hardware-aware model optimizations, improved inference frameworks, and adaptive resource management, ultimately making edge-centric AI systems more efficient and scalable.

References

- [1] Marah Abdin, Jyoti Aneja, Hany Awadalla, et al. 2024. Phi-3 Technical Report: A Highly Capable Language Model Locally on Your Phone. <https://doi.org/10.48550/arXiv.2404.14219> arXiv:cs/2404.14219
- [2] US Energy Information Administration. 2024. Electric Power Monthly, November 24. Retrieved 2024-12-18 from https://www.eia.gov/electricity/monthly/current_month/november2024.pdf
- [3] 01 AI, Alex Young, Bei Chen, et al. 2025. Yi: Open Foundation Models by 01.AI. <https://doi.org/10.48550/arXiv.2403.04652> arXiv:cs/2403.04652
- [4] Meta AI. 2024. Llama 3.2: Revolutionizing edge AI and vision with open, customizable models. Retrieved 2025-01-22 from <https://ai.meta.com/blog/llama-3-2-connect-2024-vision-edge-mobile-devices/>

- [5] Mario Almeida, Stefanos Laskaridis, Ilias Leontiadis, et al. 2019. EmBench: Quantifying Performance Variations of Deep Neural Networks across Modern Commodity Devices. In *The 3rd International Workshop on Deep Learning for Mobile Systems and Applications*. Association for Computing Machinery, New York, NY, USA, 1–6. <https://doi.org/10.1145/3325413.3329793> arXiv:1905.07346 [cs, stat].
- [6] Lenz Belzner, Thomas Gabor, and Martin Wirsing. 2024. Large Language Model Assisted Software Engineering: Prospects, Challenges, and a Case Study. In *Bridging the Gap Between AI and Reality*, Bernhard Steffen (Ed.). Springer Nature Switzerland, Cham, 355–374. https://doi.org/10.1007/978-3-031-46002-9_23
- [7] Marc Brysbaert. 2019. How many words do we read per minute? A review and meta-analysis of reading rate. *Journal of Memory and Language* 109 (Dec. 2019), 104047. <https://doi.org/10.1016/j.jml.2019.104047>
- [8] Zheng Cai, Maosong Cao, Haojong Chen, et al. 2024. InternLM2 Technical Report. arXiv:cs.CL/2403.17297
- [9] Kyunghyun Cho, Bart van Merriënboer, Caglar Gulcehre, et al. 2014. Learning Phrase Representations using RNN Encoder-Decoder for Statistical Machine Translation. <https://doi.org/10.48550/arXiv.1406.1078> arXiv:1406.1078 [cs, stat].
- [10] Hyung Won Chung, Le Hou, Shayne Longpre, et al. 2022. Scaling Instruction-Finetuned Language Models. <https://doi.org/10.48550/ARXIV.2210.11416>
- [11] Tim Dettmers, Mike Lewis, Sam Shleifer, et al. 2022. 8-bit Optimizers via Block-wise Quantization. <https://doi.org/10.48550/arXiv.2110.02861> arXiv:2110.02861 [cs].
- [12] Tim Dettmers and Luke Zettlemoyer. 2023. The case for 4-bit precision: k-bit inference scaling laws. In *Proceedings of the 40th International Conference on Machine Learning (ICML '23)*, Vol. 202. JMLR.org, Honolulu, Hawaii, USA, 7750–7774.
- [13] Jacob Devlin, Ming-Wei Chang, Kenton Lee, et al. 2019. BERT: Pre-training of Deep Bidirectional Transformers for Language Understanding. <https://doi.org/10.48550/arXiv.1810.04805> arXiv:1810.04805 [cs].
- [14] Nobel Dhar, Bobin Deng, Dan Lo, et al. 2024. An Empirical Analysis and Resource Footprint Study of Deploying Large Language Models on Edge Devices. In *Proceedings of the 2024 ACM Southeast Regional Conference (2024-04-27) (ACMSE '24)*. Association for Computing Machinery, New York, NY, USA, 69–76. <https://doi.org/10.1145/3603287.3651205>
- [15] Raspberry Pi Documentation. [n. d.]. Retrieved 2024-07-26 from <https://www.raspberrypi.com/documentation/computers/os.html#vcgencmd>
- [16] Elias Frantar, Saleh Ashkboos, Torsten Hoefler, et al. 2023. GPTQ: Accurate Post-Training Quantization for Generative Pre-trained Transformers. <https://doi.org/10.48550/arXiv.2210.17323> arXiv:2210.17323 [cs].
- [17] Aaron Grattafiori, Abhimanyu Dubey, Abhinav Jauhri, et al. 2024. The Llama 3 Herd of Models. <https://doi.org/10.48550/arXiv.2407.21783> arXiv:cs/2407.21783
- [18] Huggingface. 2024. Open LLM Leaderboard. Retrieved 2024-09-13 from https://huggingface.co/spaces/open-llm-leaderboard/open_llm_leaderboard
- [19] Andrey Ignatov, Radu Timofte, William Chou, et al. 2019. AI Benchmark: Running Deep Neural Networks on Android Smartphones. In *Computer Vision – ECCV 2018 Workshops*, Laura Leal-Taixé and Stefan Roth (Eds.). Springer International Publishing, Cham, 288–314. https://doi.org/10.1007/978-3-030-11021-5_19
- [20] MIT HAN Lab. 2023. Retrieved 2024-07-23 from <https://github.com/mit-han-lab/TinyChatEngine>
- [21] Stefanos Laskaridis, Kleomenis Katevas, Lorenzo Minto, et al. 2024. MELTing Point: Mobile Evaluation of Language Transformers. In *Proceedings of the 30th Annual International Conference on Mobile Computing and Networking (ACM MobiCom '24)*. Association for Computing Machinery, New York, NY, USA, 890–907. <https://doi.org/10.1145/3636534.3690668>
- [22] Xiang Li, Zhenyan Lu, Dongqi Cai, et al. 2024. Large Language Models on Mobile Devices: Measurements, Analysis, and Insights. In *Proceedings of the Workshop on Edge and Mobile Foundation Models (2024-06-11) (EdgeFM '24)*. Association for Computing Machinery, New York, NY, USA, 1–6. <https://doi.org/10.1145/3662006.3662059>
- [23] Ji Lin, Jiaming Tang, Haotian Tang, et al. 2024. AWQ: Activation-aware Weight Quantization for On-Device LLM Compression and Acceleration. *Proceedings of Machine Learning and Systems* 6 (May 2024), 87–100.
- [24] Jiachen Liu, Zhiyu Wu, Jae-Won Chung, et al. 2024. Andes: Defining and Enhancing Quality-of-Experience in LLM-Based Text Streaming Services. <https://doi.org/10.48550/arXiv.2404.16283> arXiv:2404.16283.
- [25] llama.cpp team. 2023. k-quants. Retrieved 2024-07-18 from <https://github.com/ggerranov/llama.cpp/pull/1684>
- [26] llama.cpp team. 2023. llama.cpp. Retrieved 2024-07-18 from <https://github.com/ggerranov/llama.cpp>
- [27] llama.cpp team. 2024. backend cpu: add online flow for aarch64 Q4_0 GEMV/GEMM kernels. Retrieved 2025-02-02 from <https://github.com/ggerranov/llama.cpp/pull/9921>
- [28] Shuming Ma, Hongyu Wang, Lingxiao Ma, et al. 2024. The Era of 1-bit LLMs: All Large Language Models are in 1.58 Bits. <https://doi.org/10.48550/arXiv.2402.17764> arXiv:2402.17764 [cs].
- [29] Stephen Merity, Caiming Xiong, James Bradbury, et al. 2016. Pointer Sentinel Mixture Models. arXiv:cs.CL/1609.07843

- [30] Zeinab Nezami, Maryam Hafeez, Karim Djemame, et al. 2024. Generative AI on the Edge: Architecture and Performance Evaluation. <https://doi.org/10.48550/arXiv.2411.17712> arXiv:cs/2411.17712
- [31] NVIDIA Corporation. 2024. Jetson Orin Nano Developer Kit Carrier Board Specification.
- [32] NVIDIA Corporation. 2024. NVIDIA Jetson Orin Nano Series Modules Data Sheet.
- [33] OpenAI. 2024. API Pricing. Retrieved 2024-12-19 from <https://openai.com/api/pricing/>
- [34] OpenAI. 2024. Gpt-4o system card. *arXiv preprint arXiv:2410.21276* (2024).
- [35] OpenAI, Josh Achiam, Steven Adler, et al. 2024. GPT-4 Technical Report. <https://doi.org/10.48550/arXiv.2303.08774> arXiv:2303.08774 [cs].
- [36] Pratyush Patel, Esha Choukse, Chaojie Zhang, et al. 2024. Splitwise: Efficient Generative LLM Inference Using Phase Splitting. In *2024 ACM/IEEE 51st Annual International Symposium on Computer Architecture (ISCA)*. IEEE, Piscataway, NJ, USA, 118–132. <https://doi.org/10.1109/ISCA59077.2024.00019>
- [37] Cheng Peng, Xi Yang, Aokun Chen, et al. 2023. A Study of Generative Large Language Model for Medical Research and Healthcare. *npj Digital Medicine* 6, 1 (Nov. 2023), 1–10. <https://doi.org/10.1038/s41746-023-00958-w>
- [38] Raspberry Pi Ltd. 2025. Raspberry Pi 5.
- [39] Vijay Janapa Reddi, Christine Cheng, David Kanter, et al. 2020. MLPerf inference benchmark. In *Proceedings of the ACM/IEEE 47th Annual International Symposium on Computer Architecture (ISCA '20)*. IEEE Press, Virtual Event, 446–459. <https://doi.org/10.1109/ISCA45697.2020.00045>
- [40] Souvika Sarkar, Mohammad Fakhruddin Babar, Md Mahadi Hassan, et al. 2024. Processing Natural Language on Embedded Devices: How Well Do Modern Models Perform?. In *Proceedings of the 15th ACM/SPEC International Conference on Performance Engineering (ICPE '24)*. Association for Computing Machinery, New York, NY, USA, 211–222. <https://doi.org/10.1145/3629526.3645054>
- [41] NVIDIA Jetson AGX Orin Series. [n. d.]. Retrieved 2025-01-26 from <https://www.nvidia.com/content/dam/en-zz/Solutions/gtcf21/jetson-orin/nvidia-jetson-agx-orin-technical-brief.pdf>
- [42] Neda Shalavi, Aria Khoshsirat, Marco Stellini, et al. 2023. Accurate Calibration of Power Measurements from Internal Power Sensors on NVIDIA Jetson Devices. In *2023 IEEE International Conference on Edge Computing and Communications (EDGE)*. IEEE, 166–170.
- [43] Penny Sweetser. 2024. Large Language Models and Video Games: A Preliminary Scoping Review. In *Proceedings of the 6th ACM Conference on Conversational User Interfaces (CUI '24)*. Association for Computing Machinery, New York, NY, USA, 1–8. <https://doi.org/10.1145/3640794.3665582>
- [44] Google team. 2024. Retrieved 2024-09-02 from https://ai.google.dev/edge/mediapipe/solutions/genai/llm_inference
- [45] Gemma Team. 2024. Gemma. <https://doi.org/10.34740/KAGGLE/M/3301>
- [46] MLC LLM team. 2023. MLC LLM. Retrieved 2024-07-23 from <https://llm.mlc.ai/>
- [47] OpenAI team. [n. d.]. Retrieved 2024-07-29 from <https://chatgpt.com/>
- [48] OpenAI team. 2024. What are tokens and how to count them? Retrieved 2024-08-23 from <https://help.openai.com/en/articles/4936856-what-are-tokens-and-how-to-count-them>
- [49] Picovoice team. 2024. PicoLLM. Retrieved 2024-07-23 from <https://github.com/Picovoice/picollm>
- [50] Ashish Vaswani, Noam Shazeer, Niki Parmar, et al. 2017. Attention is All you Need. In *Advances in Neural Information Processing Systems*, Vol. 30. Curran Associates, Inc., Red Hook, NY, USA, 5998–6008. Retrieved 2024-08-26 from https://papers.nips.cc/paper_files/paper/2017/hash/3f5ee243547dee91fbd053c1c4a845aa-Abstract.html
- [51] Hongyu Wang, Shuming Ma, Li Dong, et al. 2023. BitNet: Scaling 1-bit Transformers for Large Language Models. <https://doi.org/10.48550/arXiv.2310.11453> arXiv:2310.11453 [cs].
- [52] Guangxuan Xiao, Ji Lin, Mickael Seznec, et al. 2023. SmoothQuant: Accurate and Efficient Post-Training Quantization for Large Language Models. <https://doi.org/10.48550/arXiv.2211.10438> arXiv:2211.10438 [cs].
- [53] An Yang, Baosong Yang, Binyuan Hui, et al. 2024. Qwen2 Technical Report. <https://doi.org/10.48550/arXiv.2407.10671> arXiv:cs/2407.10671
- [54] Zheyuan Zhang, Daniel Zhang-Li, Jifan Yu, et al. 2024. Simulating Classroom Education with LLM-Empowered Agents. <https://doi.org/10.48550/arXiv.2406.19226> arXiv:cs/2406.19226
- [55] Xunyu Zhu, Jian Li, Yong Liu, et al. 2024. A Survey on Model Compression for Large Language Models. *Transactions of the Association for Computational Linguistics* 12 (Nov. 2024), 1556–1577. https://doi.org/10.1162/tacl_a_00704